PUBLICATION I

Comparison of grindability of HIPped austenitic 316L, duplex 2205 and super duplex 2507 and as-cast 304 stainless steels using alumina wheel

In: Journal of Materials Processing Technology 1996.
Vol. 62, pp. 1–9.

ELSEVIER

Journal of Materials Processing Technology 62 (1996) 1–9

Journal of Materials Processing Technology

Comparison of grindability of HIPped austenitic 316L, duplex 2205 and super duplex 2507 and as-cast 304 stainless steels using alumina wheels

Laizhu Jiang[a,*], Jukka Paro[b], Hannu Hänninen[a], Veijo Kauppinen[b], Risto Oraskari[c]

[a]*Laboratories of Engineering Materials, Helsinki University of Technology, Puumiehenkuja 3A, Espoo, Finland*
[b]*Laboratory of Workshop Technology, Helsinki University of Technology, Puumiehenkuja 3A, Espoo, Finland*
[c]*Helsinki Polytechnic Institute, Helsinki, Finland*

Received 16 September 1994; revised 21 September 1995

Industrial summary

The grinding ratios, grinding forces and surface roughnesses of HIPped austenitic (PM 316L), duplex (PM 2205) and super duplex (PM 2507) as well as as-cast (AC 304) stainless steels were measured during grinding using alumina wheels. It was observed that the grinding ratio decreased in the following order: AC 304, PM 316L, PM 2205 and PM 2507 steel, whilst the grinding force increased in the order: AC 304, PM 2205, PM 316L and PM 2507 steel. The surface roughness increased in the order: PM 316L, PM 2205, PM 2507 and AC 304 steel. It was observed also that the ground steel surfaces work-hardened in the following increasing order: AC 304, PM 316L, PM 2205 and PM 2507 steel. Abrasive plowing-wear grooves and adhesive built-up layers of alumina particles were observed on the ground surfaces of the steels, increasing in the following order: AC 304, PM 316L, PM 2205 and PM 2507 steel. Examination of the ground surface profiles of the workpieces showed that there were a considerable number of microcracks and microvoids on the ground surfaces of the steels, increasing in the following order: PM 316L, PM 2205, PM 2507 and AC 304 steel. Finally, the effects of work hardening, chemical interactions between the alumina wheel and the workpiece, as well as microcracks and microvoids, on the grindability of the stainless steels studied were investigated.

Keywords: Stainless steel; Alumina; Grinding ratio; Grinding force; Surface roughness

1. Introduction

Stainless steels are normally recognized as difficult materials to machine because of their high toughness, low thermal conductivity and high degree of work hardening. During grinding, however, the chemical interaction between a stainless-steel workpiece and a wheel, particularly an alumina wheel, may also play a crucial role in causing poor grindability. It has been reported that the poor wheel life when grinding stainless steels results mainly from a high tendency of adhesion between the workpiece and the alumina wheels [1], whilst it was also suggested much earlier that a high coefficient of friction between the workpiece and the abrasive may be responsible for a high rate of wheel wear [2]. Adhesive-wear mechanisms involve the oxidation of the workpiece and bonding between the oxidization products and the alumina [3]. It has been suggested that the chromium of stainless steel oxidizing into Cr_2O_3 could form a solid solution with Al_2O_3 and, therefore, promote bonding between stainless steels and alumina wheels. In addition, chromium would result in an increase of the friction coefficient and, therefore, in an increase of wheel wear [4].

It may be expected that not only the chemical composition, but also the microstructure of stainless steels, would exert some influences on their grindability. Although there have been some studies on the grindability of stainless steels [1,4,5], few studies have been concerned with comparison of the grindability of different types of stainless steels and with the effects of their microstructure. In this study, the grindability, i.e. the grinding ratio, the grinding force and the surface roughness of powder-metallurgically (PM) fabricated

* Corresponding author. Present address: R&D Centre, Sandvik Steel AB, 811 81 Sandviken, Sweden.

SSDI 0924-0136(95)02199-9

Table 1
Chemical compositions of the stainless steels studied (wt.%)

Code	C	Si	Mn	P	S	Cu	Cr	Ni	Mo	V	Al	N	O
PM 316L	0.05	0.68	1.44	0.022	0.009	0.19	16.7	11.0	2.7	0.11	0.021	0.12	0.012
PM 2205	0.03	0.68	1.42	0.022	0.008	0.13	22.1	5.3	3.0	0.07	0.016	0.21	0.014
PM 2507	0.03	0.30	0.30	0.035	0.009	0.16	25.0	7.0	4.0	0.08	0.020	0.30	0.015
AC 304	0.03	0.40	1.20	0.040	0.015	0.17	18.4	9.2		0.06	0.025	0.10	0.001

and hot-isostatically-pressed (HIPped) austenitic 316L, duplex 2205 and super duplex 2507 steels as well as as-cast 304 stainless steel, were measured during grinding using alumina wheels. Furthermore, the effects of the microstructure on the grindability of stainless steels were investigated.

2. Experimental

The grinding experiments were conducted on a straight surface grinder under reciprocating plunge grinding conditions. The alumina wheels used were type 43A46 GVX of 200 mm diameter and 12 mm width delivered by Norton Co., Sweden. The wheel speed was 30 m/s, the table speed was 0.25 m/s and the down feed was 0.015 mm/pass. Grinding fluid of 5% solution of Castrol no.7 in water was applied to the grinding zone at a flow rate of 2 l/min.

The workpiece materials were HIPped austenitic 316L (PM 316L), duplex 2205 (PM 2205), super duplex 2507 (PM 2507) and as-cast 304 (AC 304) stainless steels, the chemical compositions and microhardness values of the steels being given in Tables 1 and 2, respectively, and the microstructures of the steels being shown in Fig. 1(a)–(d), respectively. It can be seen that there is a considerable number of small oxide particles in the three HIPped stainless steels: much more than in AC 304 steel. Elongated ferrite phase areas are distributed in the AC 304 steel: it was impossible to measure the microhardness of the ferrite phase in this steel due to its fine structure. All the workpiece specimens were of 8 mm width, i.e., less than the wheel width, so that a recess developed in the wheel surface as a result of wheel wear, and of 200 mm length in the grinding direction. The specimens were held in place by a magnetic chuck, and positioned on the table so that the grinding marks of the ground surfaces were parallel to the longitudinal direction of the test specimens.

During grinding, the radial wheel wear was measured using a Micro-HITE surface measuring instrument. Based on these results, the grinding ratio, G, in the steady stage of wheel wear could be obtained as the ratio of the volumetric workpiece removal to the volumetric wheel wear [6]. The normal and tangential force components, F_n and F_t, during grinding were recorded with a Kistler piezo-electric grinding dynamometer and the surface roughness after grinding was measured with a Taylor surface roughness instrument. After the grinding tests, metallographic examinations and analyses of the ground surfaces and the profiles of specimens were performed by means of a scanning electron microscope (SEM) together with an energy dispersive spectroscopy (EDS). Work hardening of the specimen surface was investigated with a MHT-4 microhardness tester with a load of 20 g.

3. Results

3.1. Grinding ratio, grinding force and surface roughness

The grinding ratio, grinding force and surface roughness of four studied stainless steels are shown in Figs. 2–4, respectively. It can be seen that AC 304 steel has the highest grinding ratio followed by PM 316L, PM 2205 and PM 2507 steels while the grinding force, both the normal and tangential forces, increases in the following order: AC 304, PM 2205, PM 316L and PM 2507 steel. The surface roughness of ground stainless steels was found to increase in the following order: PM 316L, PM 2205, PM 2507 and AC 304 steel.

3.2. Work hardening of stainless steels during grinding

Work hardening of stainless steels during grinding can be seen in Fig. 5 based on the microhardness values of the workpiece as a function of distance from the ground surface. The microhardness values of the ground surfaces show that all the stainless steels tested work-hardened during grinding, if compared with the corresponding original microhardness values. In addi-

Table 2
Microhardness (HV) values of the stainless steels studied (load: 20 g)

Steel code	PM 316L	PM 2205		PM 2507		AC 304
Phase[a]	A	A	F	A	F	A
HV	250	300	330	310	340	260

[a] Phase: A-Austenite, F-Ferrite.

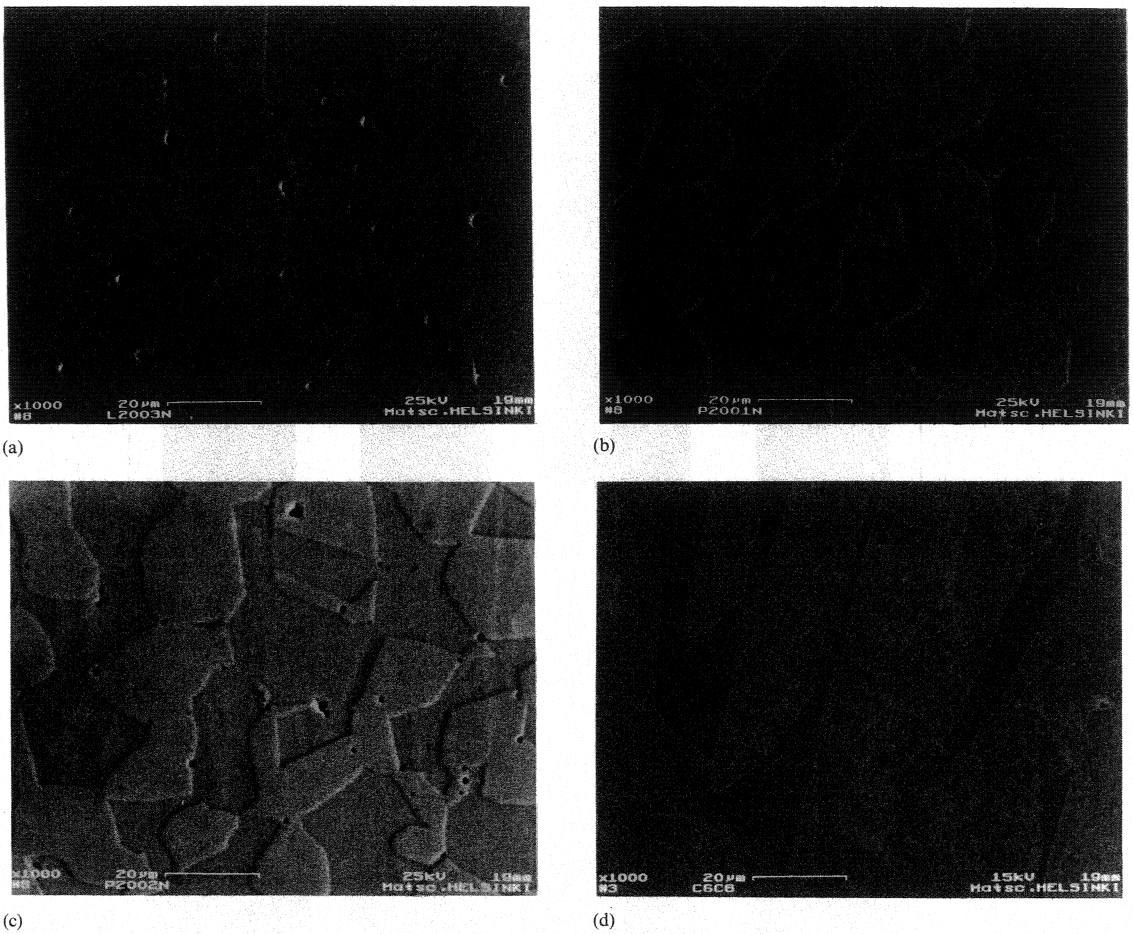

Fig. 1. BSE images of the microstructures of the stainless steels tested: (a) PM 316L steel; (b) PM 2205 steel; (c) PM 2507 steel, and (d) AC 304 steel.

tion, the austenite phase of PM 316L, PM 2205 and PM 2507 steels work-hardened more as compared with the ferrite phase of PM 2205 and PM 2507 steels and the austenite phase of AC 304 steel. Due to the elongated structure of the fine ferrite phase in AC 304 steel, it was impossible to measure the microhardness and, therefore, the work hardening of the ferrite phase of AC 304 steel.

3.3. Metallographic examination and EDS analysis of ground surface

Roughly speaking, all the ground surfaces of PM 316L, PM 2205, PM 2507 and AC 304 stainless steels, were predominantly covered by scratches and plowing wear grooves, indicating that the action of material removal of the stainless steels studied was mainly plastic flow. As an example, the morphology of the ground surface of PM 316L steel is shown in Fig. 6. In addition, the ground chip, Fig. 7, reveals that the chip-formation mechanism during grinding has been a shearing process.

Detailed SEM examinations and EDS analyses of the ground surfaces showed that there was a considerable number of alumina particles transferred from the alumina wheel to the ground surface, increasing in the following order: AC 304, PM 316L, PM 2205 and PM 2507 steel. As an example, the morphology of the ground surface and the element distribution on the surface of PM 2507 steel are shown in Fig. 8. It can be seen easily that the alumina particles adhere to the ground surface. There is some enrichment of molybdenum and silicon, some depletion of chromium and iron and a greater depletion of nickel and manganese at the sites of alumina particles, indicating that the bonding mechanism between the alumina wheel and the stainless

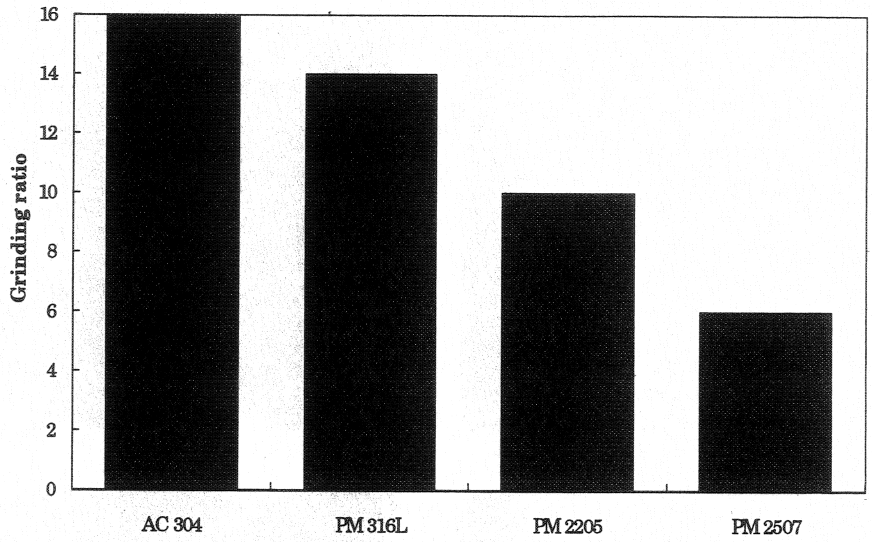

Fig. 2. Grinding ratio of stainless steels ground with alumina wheels.

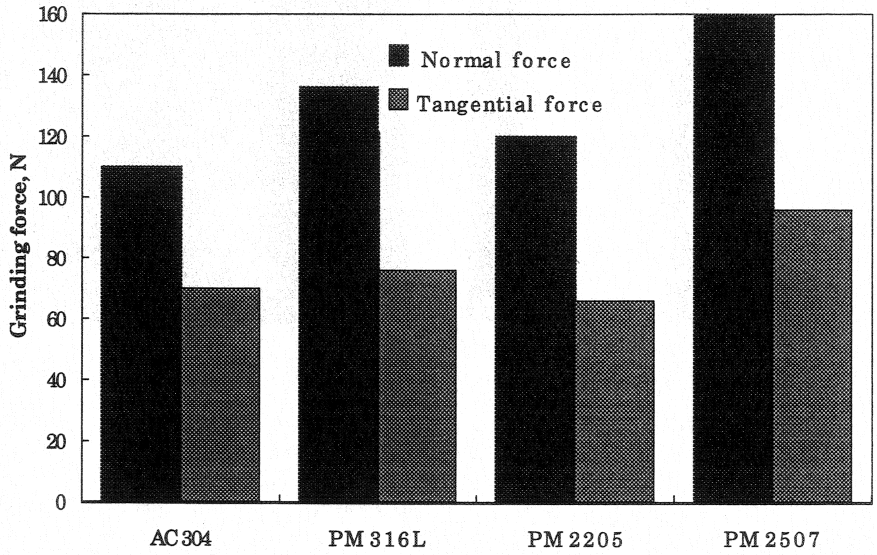

Fig. 3. Normal and tangential forces when grinding stainless steels using alumina wheels.

steels was due to the oxidation of mainly molybdenum and silicon and the consequent bonding between these oxides and Al_2O_3 from the alumina wheel.

3.4. Metallographic examination of ground surface profiles

Macrographs of the ground surface profiles of the steels studied are shown in Fig. 9(a)–(d). It can be seen that the ground surface of PM 316L steel is the smoothest, followed by those of PM 2205, PM 2507 and AC 304 steel.

Alumina particles, together with oxidation products of mainly molybdenum and silicon, were observed also in the profiles of the ground surfaces, Fig. 10, indicating further that some alumina particles are transferred from the alumina wheel to the stainless-steel surface during grinding.

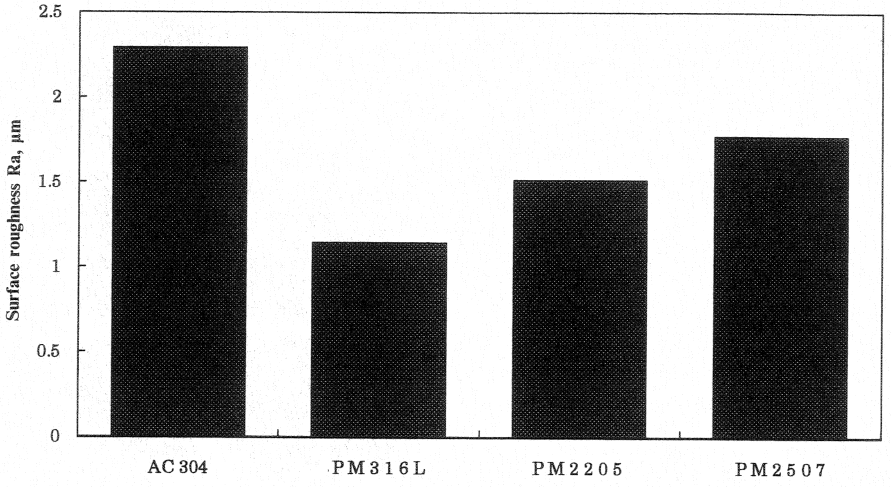

Fig. 4. Surface roughness R_a of stainless steels ground with alumina wheels.

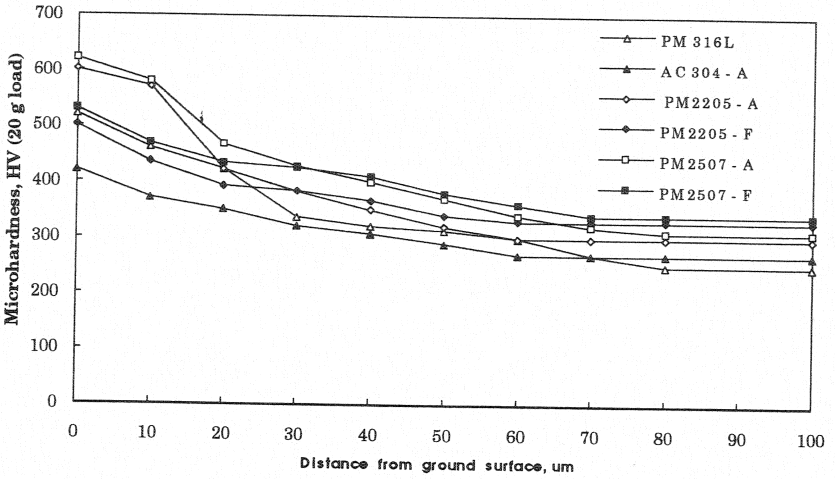

Fig. 5. Work hardening of stainless steels during grinding.

There was also a considerable number of microcracks and microvoids initiated on the ground surface of the steels studied. As an example, Fig. 11 shows microcracks and microvoids on the ground surface of AC 304 steel. These microcracks and microvoids may lead to the fracture of pieces of materials from the workpiece. Furthermore, it was observed that the density of microcracks and microvoids on the ground surface of the steels increased in the following order: PM 316L, PM 2205, PM 2507 and AC 304 steel.

There are two possible mechanisms for the formation of microcracks and microvoids on the ground surfaces of the steels studied.

1. Oxide inclusion initiation. During grinding, the hard oxide inclusions in the workpiece do not deform plastically, whilst the stainless steel matrix shows marked plastic flow. This mismatch of the strain between the hard oxide inclusions and the much softer matrix results in highly localized stresses at the interface leading to de-cohesion of the interface, microcracks and microvoids then being formed, as shown in Fig. 12 (a) and (b).

2. Mismatch of the deformability between the ferrite and the austenite phases. This mismatch results in highly localized stresses in the phase boundary leading to de-cohesion of the interface between the ferrite and the austenite phases and consequently to the formation of microcracks and microvoids, Fig. 13.

In PM 316L steel, only mechanism 1 was active, whilst in the rest of the steels studied, both mechanisms 1 and 2 were active in the formation of microcracks and microvoids on the ground surfaces.

4. Discussion

Due to the observed surface work hardening of ground stainless steels and the chemical interaction between them and the alumina wheels, it may be supposed that both attrition and adhesive wear occurs in alumina wheels when grinding stainless steels. Regarding the attrition wear, it may be expected that the wheel wear is the lowest and grinding ratio the highest when grinding AC 304 steel, followed by PM 316L, PM 2205 and PM 2507 steel, if considering the microhardness values of the ground steels. In addition, the presence of small hard oxide particles in the three HIPped stainless steels causes more excessive abrasive wear of alumina wheels as compared with that when grinding AC 304 steel. The adhesive wear was found to be dependent on the chemical interaction between the wheel and the workpiece. Due to the chemical interaction between the alumina wheel and the ground stainless steel, PM 2507 steel has the highest tendency to the adherence of alumina particles from the wheel, followed by PM 2205, PM 316L and AC 304 steels if the contents of molybdenum and silicon in the workpiece materials are considered. This was verified also by observations of the number of alumina particles on the ground surfaces of the steels studied. Based on the overall consideration of both attrition and adhesive wear, together with abrasive wear, it can be concluded that the wheel wear was the lowest and the grinding ratio the highest when grinding AC 304 steel, followed by PM 316L, PM 2205 and PM 2507 steels, while using alumina wheels.

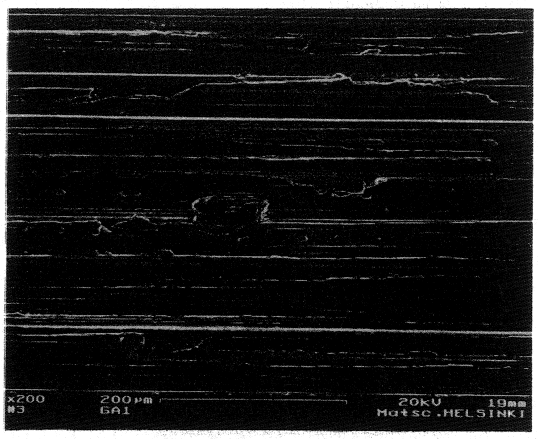

Fig. 6. Ground surface morphology of PM 316L steel showing scratches and plowing grooves.

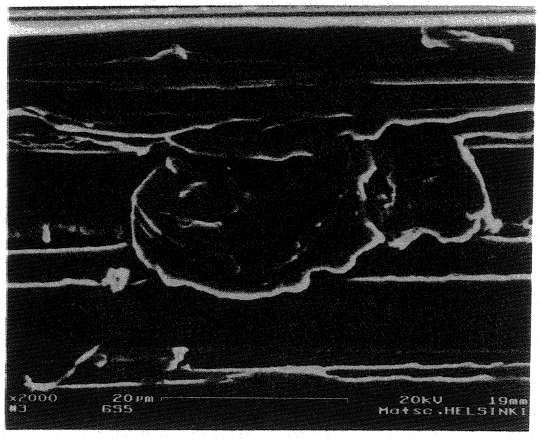

Fig. 7. Curled chip on the ground surface of PM 2507 steel showing a fine lamella structure formed as a result of shear instability.

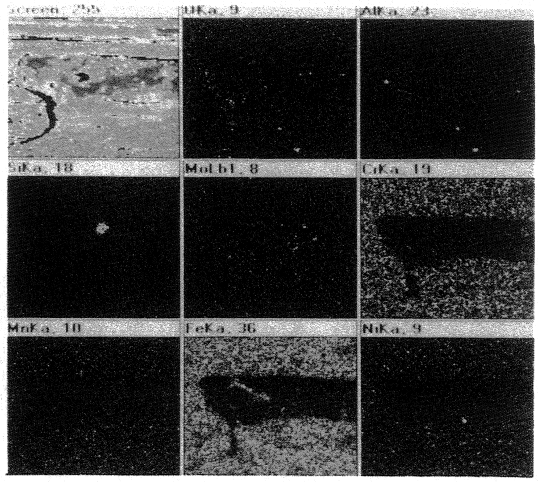

Fig. 8. EDS analyses of element distribution on the ground surface of PM 2507 steel.

The grinding forces were dependent not only on the work hardening of the workpiece, but also on the density of microcracks and microvoids forming during grinding of the workpiece. It was observed that the microhardness values of the ground steel surfaces increased in the following order: AC 304, PM 316L, PM 2205 and PM 2507 steel. The corresponding grinding forces would be expected to increase in the same order if considering only the effects of work hardening of the workpiece during grinding. However, the experimental results showed that the grinding forces increased in the order: AC 304, PM 2205, PM 316L and PM 2507 steel. The actual order of grinding forces when grinding PM 316L and PM 2205 steels may be due to the effects of microcracks and microvoids on the ground surface. It has been reported that the presence of microcracks and microvoids in the shear zone would lead to a reduction of cutting force during turning [7]: a similar conclusion may be applicable for grinding. In these tests, it was found that the area density of microcracks and microvoids on the ground surface of PM 2205 steel was much greater than that of PM 316L steel, resulting in

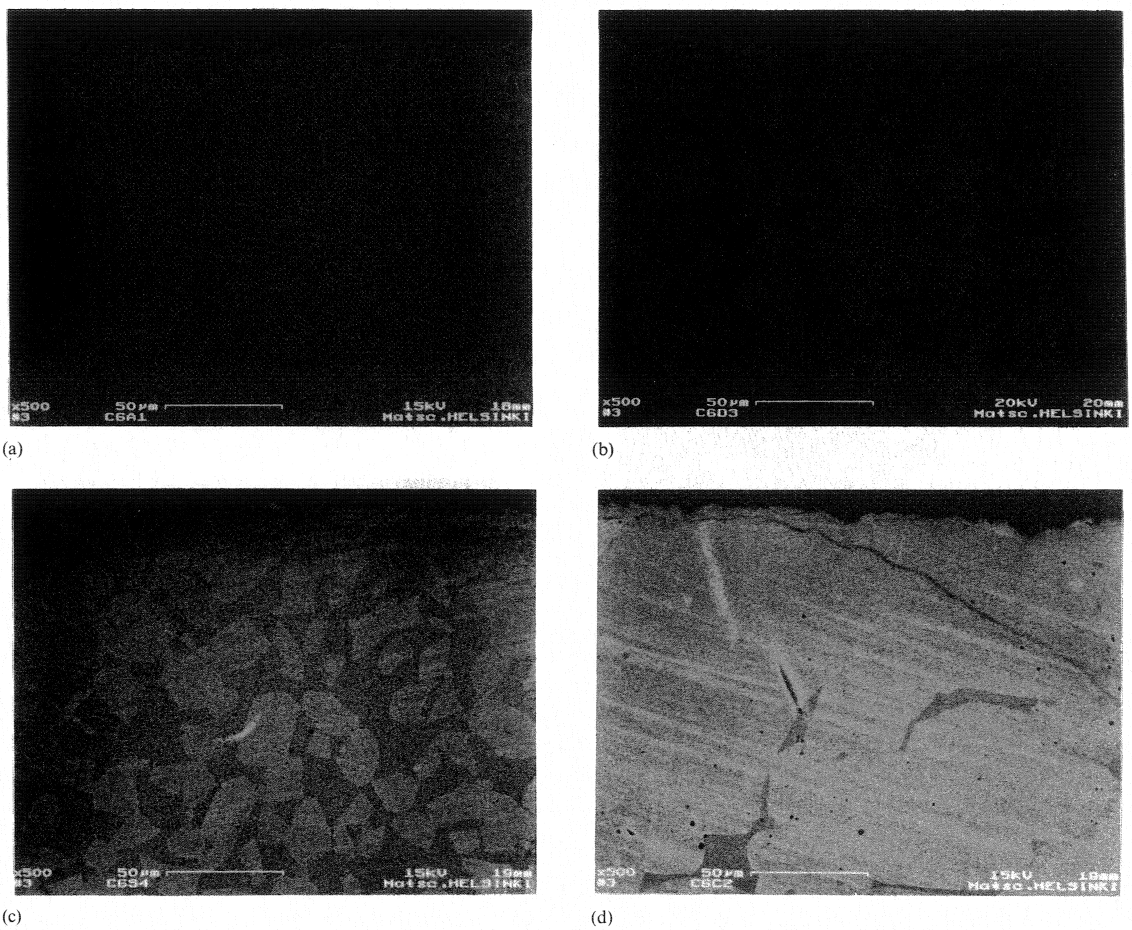

(a) (b)

(c) (d)

Fig. 9. BSE images of the morphology of the profiles of the ground surface of the stainless steels tested: (a) PM 316L steel; (b) PM 2205 steel; (c) PM 2507 steel, and (d) AC 304 steel.

the grinding forces when grinding PM 316L steel being greater as compared with those when grinding PM 2205 steel.

The surface roughness of the ground samples was dependent predominantly on the area density of micro cracks and microvoids on the ground surface. It was observed in these experiments that the area density increased in the following order: PM 316L, PM 2205, PM 2507 and AC 304 steel. There was no doubt that the density of microcracks and microvoids on the ground surface of PM 316L steel was the lowest because only oxide inclusions were responsible for the formation of microcracks and microvoids, whilst in addition to the oxide inclusions also the mismatch of strain between the ferrite and the austenite phases was responsible for the formation of microcracks and microvoids in PM 2205, PM 2507 and AC 304 steels. Due to the elongated shape of the ferrite phase in AC 304 steel, it may be expected that a higher stress concentration would arise and accordingly more (area density) microcracks and microvoids would be initiated when grinding AC 304 steel as compared with that when grinding both PM 2205 and PM 2507 steels. As an example, microcracks and microvoids on the ground surface of AC 304 steel are shown in Fig. 14. The area density of microcracks or microvoids initiated by the elongated ferrite phase in AC 304 steel was much higher as compared with that in PM 2507 steel (Fig. 13). Due to the higher alloy content of PM 2507 steel, the ductility and toughness of the ferrite phase is lower and the tendency for microcracks and microvoids to form is higher as compared with that of PM 2205 steel. Accordingly, it is understandable that surface roughness of ground steels increases in the following order: PM 316L, PM 2205, PM 2507 and AC 304 steel, i.e., in the same order as the density of microcracks and microvoids on the ground surface increases.

5. Conclusions

The grindability of PM 316L, PM 2205, PM 2507 and AC 304 stainless steels was examined in terms of grinding ratio, grinding force and surface roughness using alumina wheels. It was observed that the grinding ratio decreased in the following order: AC 304, PM 316L, PM 2205 and PM 2507 steel; the grinding force increased in the following order: AC 304, PM 2205, PM 316L and PM 2507 steel, and the surface roughness increased in the following order: PM 316L, PM 2205, PM 2507 and AC 304 steel.

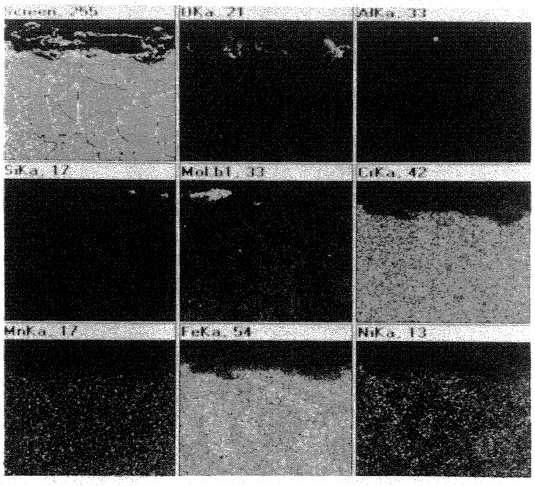

Fig. 10. EDS mapping analyses of the ground surface of PM 2507 steel.

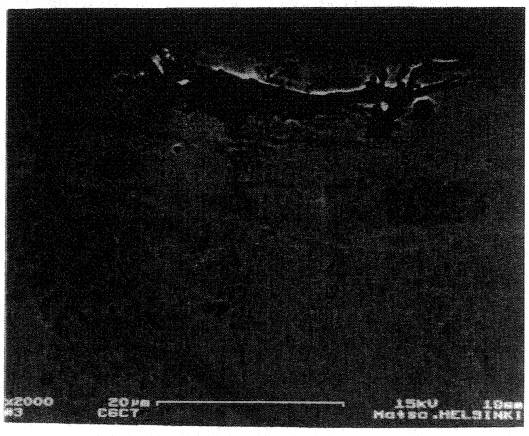

Fig. 11. Microcracks and microvoids on the ground surface of AC 304 steel.

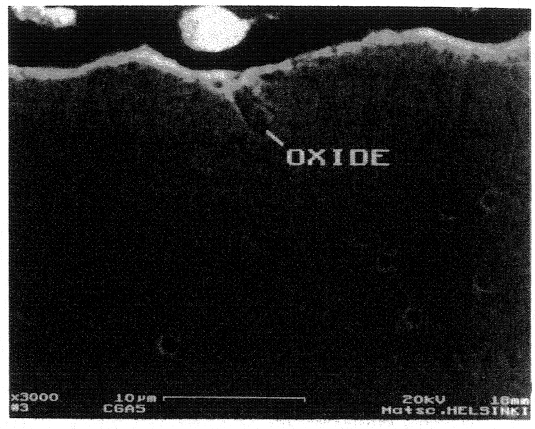

(a)

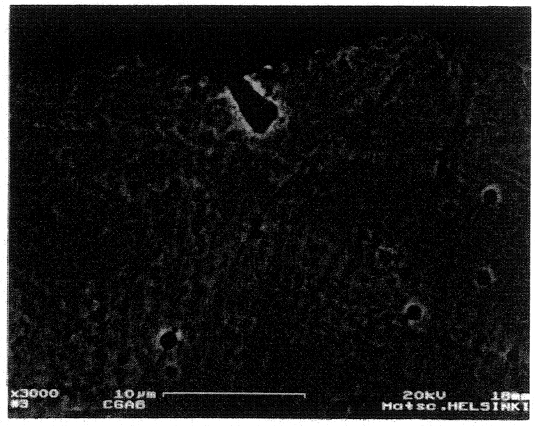

(b)

Fig. 12. Microvoid initiaton by oxide inclusions on the ground surface of PM 316L steel: (a) secondary electron image, and (b) back-scattered electron image.

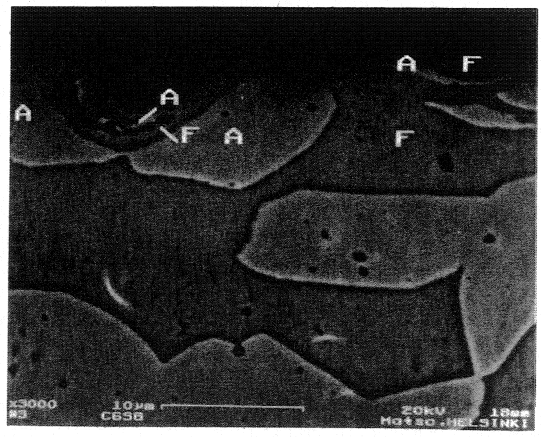

Fig. 13. Microcrack and microvoid initiation at the phase boundary between the austenite and the ferrite phases in PM 2507 steel.

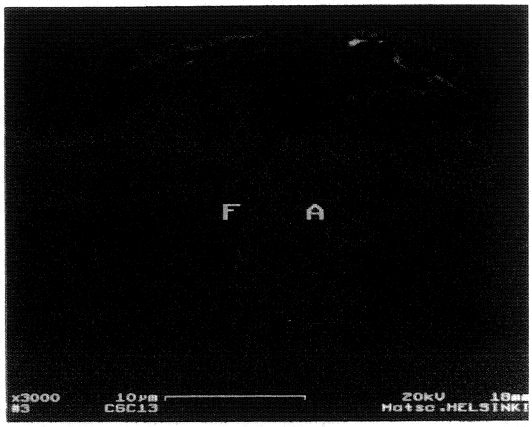

Fig. 14. Back-scattered electron image of microcracks and microvoids on the ground surface of AC 304 steel.

The work-hardening behaviour of stainless steels during grinding increased in the following order: AC 304, PM 316L, PM 2205 and PM 2507 steel. Alumina particles transferred from alumina wheels were detected on the ground surfaces. The mechanism of transfer may be the oxidation of mainly molybdenum and silicon of stainless steels and the subsequent bonding of alumina and these oxidation products. In addition, a considerable number of microcracks and microvoids was detected on the ground surfaces of the steels in the following increasing order: PM 316L, PM 2205, PM 2507 and AC 304 steel.

Acknowledgements

The financial support from TEKES (Technology Development Centre of Finland) is greatly acknowledged. Thanks are due to Rauma Materials Technology Co., Tampere, for supplying the workpiece materials. The assistance of Mr Alpo Hakola in Laboratory of Workshop Technology, Helsinki University of Technology, in the grinding tests is deeply appreciated. Active interest in this project from Dr Jari Liimatainen, Rauma Materials Technology Co., is also acknowledged.

References

[1] S. Yossifon and C. Rubenstein, *J. Eng. Ind.*, *103* (1981) 144–155.
[2] W.A. Mohun, *J. Eng. Ind.*, *84* (1962) 466–482.
[3] R. Komanduri, *Ann. CIRP*, *2* (1976) 191–196.
[4] K. Miyoshi and D.H. Buckley, *Wear*, *82* (1982) 197–211.
[5] S. Yossifon and C. Rubenstein, *Ann. CIRP*, *31* (1982) 225–228.
[6] S. Malkin, *Grinding Technology: Theory and Application of Machining with Abrasives*, Ellis Horwood, Chichester, UK, 1989.
[7] L.H.S. Luong, *Met. Technol.*, *7* (1980) 465–470.